Nat. Hazards Earth Syst. Sci. Discuss., https://doi.org/10.5194/nhess-2018-231
Manuscript under review for journal Nat. Hazards Earth Syst. Sci.
Discussion started: 14 August 2018

Natural Hazards and Earth System Sciences
Discussions

Stochastic generation of spatially coherent river discharge peaks for large-scale, event-based flood risk assessment.

Dirk Diederen[1], Ye Liu[1], Ben Gouldby[1], Ferdinand Diermanse[2], and Sergiy Vorogushyn[3]

[1]HR Wallingford, Crowmarsh Gifford, United Kingdom
[2]Deltares, Delft, Netherlands
[3]GFZ German Research Centre for Geosciences, Potsdam, Germany

Correspondence to: Dirk Diederen (d.diederen@hrwallingford.com)

Abstract. Flood risk assessments are required for long-term planning, e.g. for investments in infrastructure and other urban capital. Vorogushyn et al. (2018) call for new methods in large-scale 'Flood Risk Assessment' (FRA) to enable the capturing of system interactions and feedbacks. With the increase of computational power, large-scale, continental FRAs have recently become feasible (Ward et al., 2013; Alfieri et al., 2014; Dottori et al., 2016; Vousdoukas, 2016; Winsemius et al., 2016; Paprotny et al., 2017).

Flood events cause large damages worldwide (Desai et al., 2015). Moreover, widespread flooding can potentially cause large damage in a short time window. Therefore, large-scale (e.g. pan-European) events and for instance maximum probable damages are of interest, in particular for the (re)insurance industry, because they want to know the chance of their widespread portfolio of assets getting affected by large-scale events (Jongman et al., 2014).

Using a pan-European data set of modelled, gridded river discharge data, we tracked discharge waves in all major European river basins. We synthetically generated a large catalogue of synthetic, pan-European events, consisting of spatially coherent discharge peak sets.

1 Introduction

1.1 General approaches to FRA

Typically, for FRAs a chain of models is applied, covering the entire risk cascade from hazardous extreme events down to flood damages or casualties resulting from inundation (e.g. expected annual damage, loss of life). The chain can be run in continuous mode (Cameron et al., 1999; Boughton and Droop, 2003; Borgomeo et al., 2015; Falter et al., 2015), or with separate events (Vorogushyn et al., 2010; Gouldby et al., 2017). Event-based model runs require initial conditions for each event, introducing the challenge to include the influence of antecedent conditions in sequences of events (Berthet et al., 2009; Schröter et al., 2015). Running the models in continuous mode has the advantage that pre-event conditions such as e.g. soil moisture state

Nat. Hazards Earth Syst. Sci. Discuss., https://doi.org/10.5194/nhess-2018-231
Manuscript under review for journal Nat. Hazards Earth Syst. Sci.
Discussion started: 14 August 2018

or pre-event river flow are explicitly simulated by the model chain. Continuous simulation can be, however, computationally much more expensive.

Following the definition of risk (Field, 2012), simply put as probability of damage, FRA requires an approximation of the risk curve under stationary climate conditions and a current distribution of asset values. The risk curve represents the probability of damages and is approximated by the evaluation of a comprehensive set of hazard scenarios, which represent a series of flood events in space and time. The latter are typically generated as synthetic data with models conditioned on observations.

Fluvial flood events occur where water escapes the river in an uncontrolled fashion. Such flood events are driven by discharge waves, which cause the exceedance of bankful conditions or cause dikes to fail. Each discharge wave occurs in a particular time window, which varies for each location. With an increasing spatial scale, events overlap in time and merge into a space-time continuum. For a large-scale FRA, the challenge arises how to define and simulate large-scale, synthetic river discharge events, retaining their statistical properties in space (spatial dependence/coherence).

1.2 Flood events in space and time

1.2.1 The challenge of event definition

River discharge events show a wave-like behaviour. Travel times of discharge waves (i.e. time lags between flow peaks at different locations) in large river basins can be long. Therefore, a new discharge wave may be generated upstream, while the previous discharge wave has not yet reached the river mouth. Furthermore, discharge waves in river basins are triggered by atmospheric events that may span across multiple river basins. Finally, discharge waves in different river basins may be related to a single atmospheric event, but do not occur at the same time. Hence, considering large-spatial scales, going beyond the boundaries of a single catchment, imposes a challenge on the definition of large-scale, river discharge events.

1.2.2 Blocks vs dynamic events

We distinguish between two groups of event identification methods: methods based on time blocks and methods based on dynamic events. Using blocks, events are defined within fixed time windows and described by their statistical properties, e.g. annual maximum peak flows. The main advantage of blocks is its simplicity, allowing statistical properties to be directly derived.

Dynamic events are defined as events in space-time windows, which are based on the discharge values. This may result in a spatially varying time window for each event. As described above, at large spatial scales small-scale events at different locations may overlap and form one single long-lasting spatio-temporal event. Hence, a practical definition of space-time windows is required.

Nat. Hazards Earth Syst. Sci. Discuss., https://doi.org/10.5194/nhess-2018-231
Manuscript under review for journal Nat. Hazards Earth Syst. Sci.
Discussion started: 14 August 2018

Natural Hazards and Earth System Sciences
Discussions

Table 1. L1-6 are different locations. Sets 1-4 describe a discharge event. Generally, dynamic discharge events do not occur at all locations, such that peaks (P) cannot be identified for all locations. Therefore, auxiliary values (A) have to be used to fill in the gaps.

	L1	L2	L3	L4	L5	L6
Set 1	P	P	P	P	A	A
Set 2	A	P	P	A	P	A
Set 3	P	A	P	P	P	A
Set 4	P	P	A	P	P	P

1.2.3 Handling dynamic events in a statistical event generator

Historically, observations have been made at specific locations, e.g. discharge gauge stations at certain locations along rivers [cite]. Therefore, most event identification methods are designed for local frequency analysis of discharge waves, starting with the identification of 'local events', i.e. events at certain locations.

In reality, discharge waves will not occur at all gauged locations within a reasonable time window. The larger the spatial scale in which discharge waves are considered, the more likely it is they are spread out in time. Therefore, an extraction of a dynamic event from a space-time continuum, trying to obtain local peaks for all locations, will lead to a matrix of incomplete peak sets. Gaps emerge at locations, where no event occurs within a reasonable time window. Current statistical methods for multivariate event generation cannot handle a matrix with missing components (Keef et al., 2009). Therefore, 'auxiliary values', i.e. values that do not represent flood wave peaks, are required in order to fill up the gaps (see Table 1). Different methods exist to assign auxiliary values, for different purposes. Gouldby et al. (2017) analysed different coastal flood variables with an event-based approach, where they adopted concurrent values at all locations where particular thresholds had not been exceeded (i.e. no local event). Keef et al. (2009) relaxed the time constraint, where they considered the values at all locations within a -3 to +3 days time window.

In this study, we analysed pan-European discharge waves in the space-time continuum, which are characterised by significant time lags between peaks at multiple locations. We applied a new method of dynamic event identification where we aimed to capture discharge events in each major European river basin, after which we used a block-based method to merge them to spatially-coherent, pan-European events. The so-derived events were analysed and used to parameterise a stochastic event generation model. The statistical properties of synthetic events produced by the event generator were finally compared to those of the observed.

2 Data and Framework

In this study we used a gridded discharge data set covering major river networks in Europe (Alfieri et al., 2014). This dataset resulted from a hydrological model driven by a climate re-analysis data set for the period 1990 to 2015 and has a spatial

Nat. Hazards Earth Syst. Sci. Discuss., https://doi.org/10.5194/nhess-2018-231
Manuscript under review for journal Nat. Hazards Earth Syst. Sci.
Discussion started: 14 August 2018

Natural Hazards and Earth System Sciences
Discussions

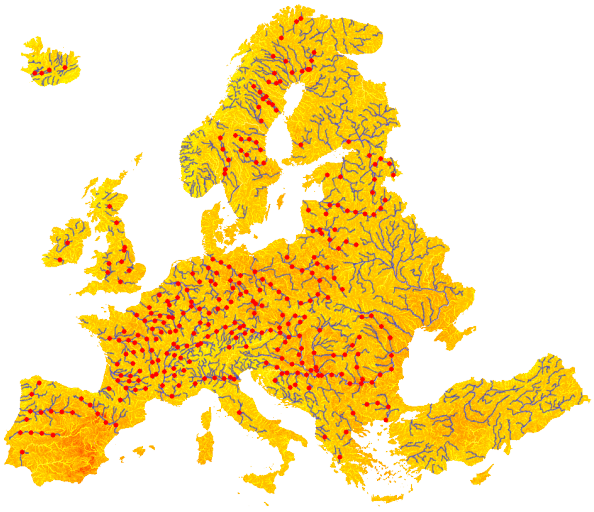

Figure 1. The network of major European rivers and a subset of 298 representative locations (red dots).

resolution of 5x5km and a daily temporal resolution. A high temporal resolution is critical for river discharge waves to be tracked in the extended river networks (Fig.(1). In order to keep the computational costs reasonable, the network was reduced to the major streams and tributaries. For high-order small streams to be included, even higher temporal resolution (hourly) would be required for wave tracking.

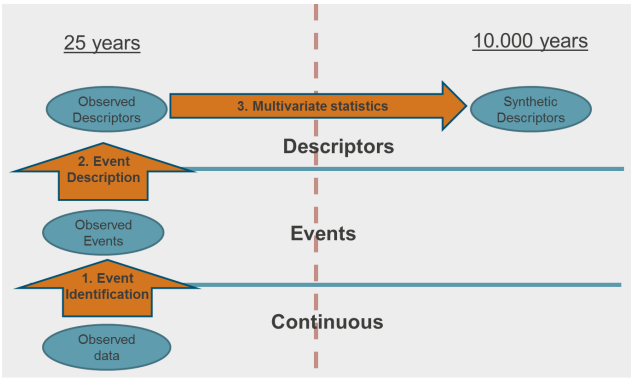

Figure 2. Framework.

The framework for the generation of synthetic peak sets consists of three consecutive steps, see Fig.(2). First, we identified pan-European events in the continuous data on the entire river network. To achieve this, we started by identifying local events (single location), for which we applied a new method of time series analysis, 'Noise Removal' (NR), at every location in the

Nat. Hazards Earth Syst. Sci. Discuss., https://doi.org/10.5194/nhess-2018-231
Manuscript under review for journal Nat. Hazards Earth Syst. Sci.
Discussion started: 14 August 2018

Natural Hazards and Earth System Sciences
Discussions

river network. These local events were then connected to neighbouring locations to obtain river basin events, to be subsequently merged to pan-European events, which span across multiple river basins.

Second, to reduce the dimension (number of locations) for statistical analysis while trying to maintain an acceptable spatial coverage, we selected 298 representative locations within the network of major European rivers, see Fig.(1). At these representative locations, we described the local discharge events by their peaks, where peaks on different representative locations were connected using the pan-European events.

Third, we fitted a multivariate extreme value model to the series of discharge peaks covering 25 years retaining the observed spatial correlation structure. The fitted statistical model was finally used to simulate a large set of synthetic discharge peaks (comprising 10,000 synthetic years), characterised by spatial coherence.

3 Events

3.1 Single-location events

When studying discharge waves moving through the river network by 'extremeness-per-location', a complex behaviour can be expected. Relatively extreme events upstream may become less extreme moving downstream when the lower part of the river basin is not activated. Or, in contrast, relatively non-extreme events at different upstream branches can generate a relatively extreme event at confluences downstream due to wave superposition. However, when using the popular 'Peaks-Over-Threshold' method (POT), all events below a particular threshold are dropped. Therefore, we developed a new noise removal algorithm to capture local events which manages to eliminate small local peaks which are part of a bigger event (noise), while retaining small events which may be spatially connected to larger events upstream or downstream. This is a key feature to the wave tracking which will be explained in Sect.[3.2].

The prodecure of NR is as follows. First, we identified all local minima μ and maxima M, defined as the points where the sign of the increment changes from positive to negative and vice versa. We started from a local minimum and ended with a local minimum, see Fig.(3a). Second, we identified small perturbations as noise and removed them, where we applied the following procedure:

1. Define a series $Y = (\mu_1, M_1, \mu_2, .., \mu_{n-1}, M_{n_M}, \mu_{n_\mu})$ and calculate $dY = \left|\mu_1 - M_1, M_1 - \mu_2, .., M_{n_M} - \mu_{n_\mu}\right|$.
2. Either calculate the 'NR value window' $\delta_y = f_y \times max(dY)$, where f_y is a fraction to set, or set δ_y directly.
3. Select the smallest difference in value $dY_i = min(dY)$. If $dY_i < \delta_y$, remove Y_{i-1} and Y_i from Y, then recalculate dY. Repeat this step until there is nothing left to remove.

An example of the NR value window filtering is displayed in Fig.(3b). Third, we made sure that two local minima were not too close in time, for which we applied the following procedure:

1. Define a series $T = (t_{\mu_1}, t_{\mu_2}, .., t_{\mu_n})$ and calculate $dT = \left(t_{\mu_2} - t_{\mu_1}, t_{\mu_3} - t_{\mu_2}, .., t_{\mu_n} - t_{\mu_{n-1}}\right)$.

Nat. Hazards Earth Syst. Sci. Discuss., https://doi.org/10.5194/nhess-2018-231
Manuscript under review for journal Nat. Hazards Earth Syst. Sci.
Discussion started: 14 August 2018

2. Either calculate the 'NR time window' $\delta_t = f_t \times max(dT)$, where f_t is a fraction to set, or set δ_t directly.

3. Select the smallest difference in time $i = argmin_i dT_i$. If $\mu_{i-1} < \mu_i$, $j = i$, else $j = i-1$. If $M_{j-1} < M_j$, $k = j-1$, else $k = j$. Remove Y_{2j-1}, Y_{2k} and T_j, then recalculate dT. Repeat this step until there is nothing left to remove.

An example of the time window filtering is displayed in Fig.(3c). Fourth, for each location we defined the day of each remaining maximum ± 1 day as a local discharge event.

We set the NR value window fraction relatively low ($f_y = 0.01$), such that many small local events were retained. However, by setting the fraction low, small perturbations (noise) made it difficult to spatially separate events. This was ameliorated by using the NR time window $f_t = 10days$, ensuring a minimal time between local minima. These NR parameters were identified by trial and error, which will be explained in Sect.[3.2].

3.2 River basin events

River discharge waves generally propagate through the network in downstream direction, introducing time lags between the moments the waves pass at different locations. Time lags are difficult to estimate, because the celerity of river discharge waves can be highly nonlinear. Wave celerity is a function of hydraulic depth and changes in a nonlinear way when overbank flow occurs and floodplains become inundated. When using gauge data (point-observations), combining local events to events that span multiple locations, time lags are typically addressed using time windows. The gridded data set used in this study allowed us to try a new method to combine local events to river basin events, which we refer to as 'wave tracking'. Each location in the river network is physically connected to its neighbouring locations, therefore allowing waves to be tracked throughout the entire river network. Wave tracking is robust to nonlinearities in the wave celerity, and therefore it allows to better address time lags, so that, when we compare peaks at different locations in Sect.[4], we make sure they are of the same discharge wave.

To track river discharge waves, we applied the following procedure. First, we separated local events by applying NR to time series at every location in the river network, where of each local event we retained the day of the peaks ± 1 day. Second, we identified separate events per river branch by capturing the polygons in the branch's space-time image, see Fig.(4). The settings of the NR were adjusted by trial and error to try to obtain consistent polygons in space (low noise removal), but separated in time (high noise removal). Third, we merged the events of different river branches based on overlap of event time coordinates at the confluences.

3.3 Pan-European events

Precipitation events, which are the main driving source of river discharge events, span across different river basins. Therefore, large discharge events in adjacent river basins are likely to be correlated. To account for this correlation, we had to define events that included discharge waves across different river basins (in this study pan-European events). Since discharge waves do not span across different river basins (by definition), such events should be connected to each other in a different way. Discharge waves in different basins are not synchronised, which adds additional complexity. In order to construct pan-European events,

Nat. Hazards Earth Syst. Sci. Discuss., https://doi.org/10.5194/nhess-2018-231
Manuscript under review for journal Nat. Hazards Earth Syst. Sci.
Discussion started: 14 August 2018

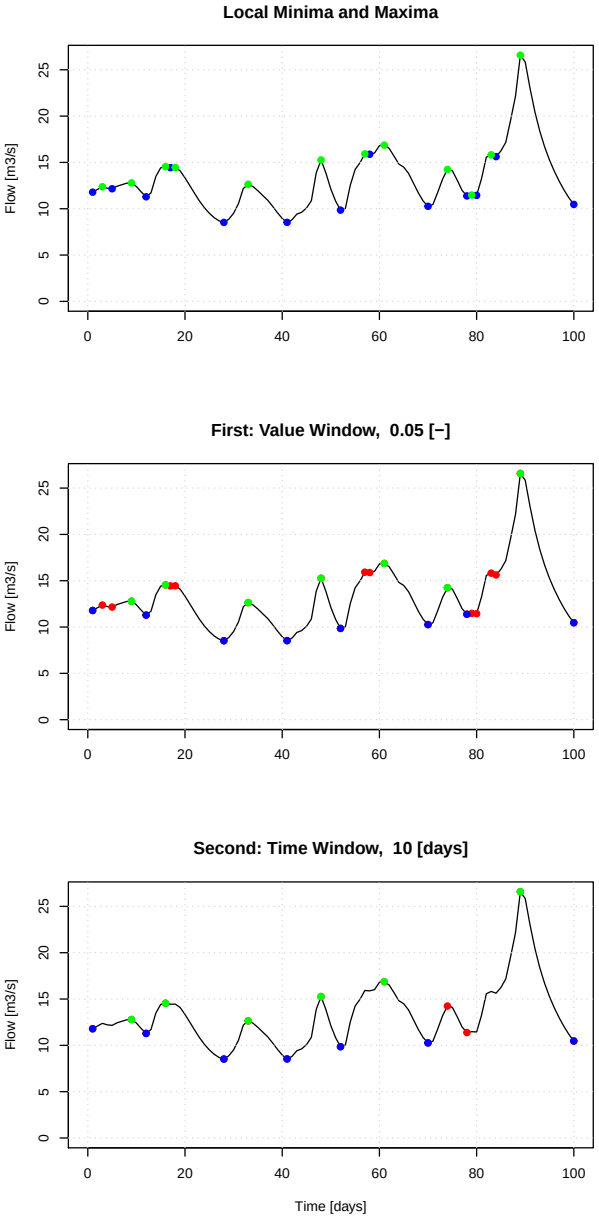

Figure 3. An example of the noise removal method. Blue dots are local minima, green dots are local maxima, red dots are local minima or maxima that are identified as 'noise' and are removed.

which on one hand consider discharge waves in river basins and on the other hand account for trans-basin dependency, we propose a combined approach of wave tracking and 'global time windows'.

Nat. Hazards Earth Syst. Sci. Discuss., https://doi.org/10.5194/nhess-2018-231
Manuscript under review for journal Nat. Hazards Earth Syst. Sci.
Discussion started: 14 August 2018

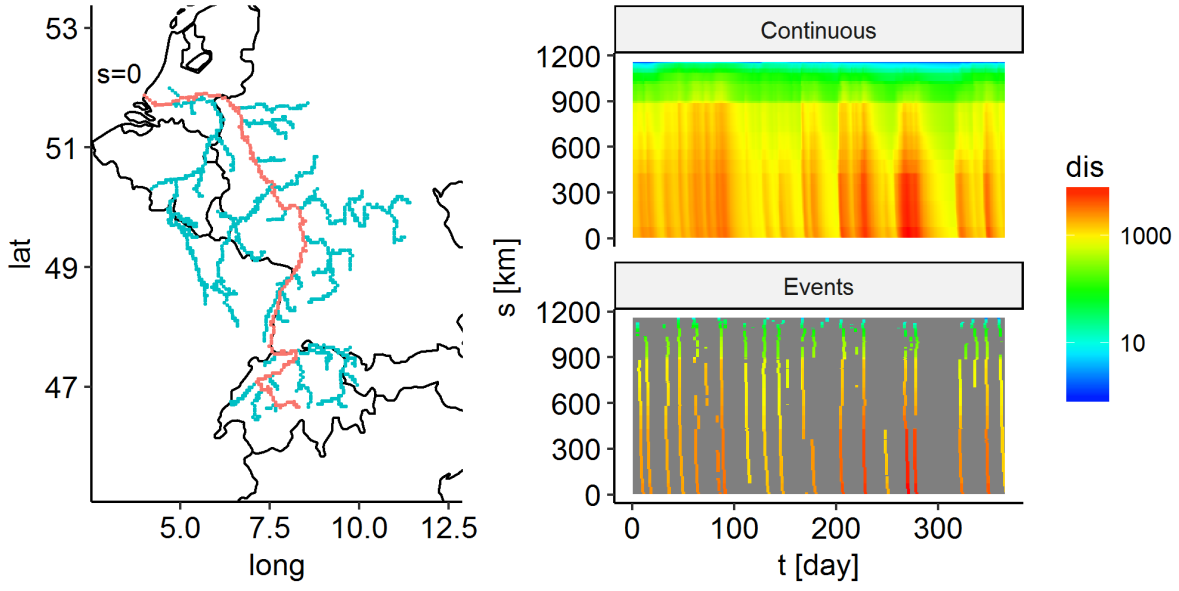

Figure 4. a) A particular branch of the river Rhine. b) The continuous discharge data on the river branch, where the river mouth is located at $s = 0km$ and the head water is located around $s = 1100km$. c) Events on the river branch. The polygons (i.e. coloured islands of data separated by the grey field) are discharge waves moving through the river branch.

The following procedure was adopted. First, we set up the global time windows. As soon as the first peak was detected at any location in the river network, a global time window was opened, to be subsequently closed after 21 days. Continuing after the last global time window, this procedure was repeated and resulted in 428 global time windows in the period 1990-2015 (i.e. 428 pan-European events). Second, to each global time window we assigned complete, tracked discharge waves. To do this, we let each discharge wave be represented by its first time coordinate, i.e. the day when the discharge wave started somewhere (upstream) in the river basin. The discharge wave was then assigned to the global time window in which this day occurred. If, per river basin, multiple discharge waves were assigned to a particular global time window, we only retained the discharge wave with the largest discharge value. An example of a pan-European event is displayed in Fig.(5).

The length of the global time window of 21 days was found by a trial and error procedure, considering the following trade-off. To each pan-European event, one river basin event should be assigned, which in an ideal world would give one local event for each representative location. However, depending on the window length, multiple river basin events may be assigned or there may be no river basin event to assign to the global time window. Therefore, when applying a relatively large global time window, the frequency of discharge waves in river basins with high frequencies will be underestimated, whereas a relatively small global time window will lead to a large percentage of missing local events at the representative locations. Since we were dealing with a large-scale analysis, the percentage of missing events at representative locations was relatively large and therefore decisive for the choice of a relatively large global time window (21 days).

Nat. Hazards Earth Syst. Sci. Discuss., https://doi.org/10.5194/nhess-2018-231
Manuscript under review for journal Nat. Hazards Earth Syst. Sci.
Discussion started: 14 August 2018

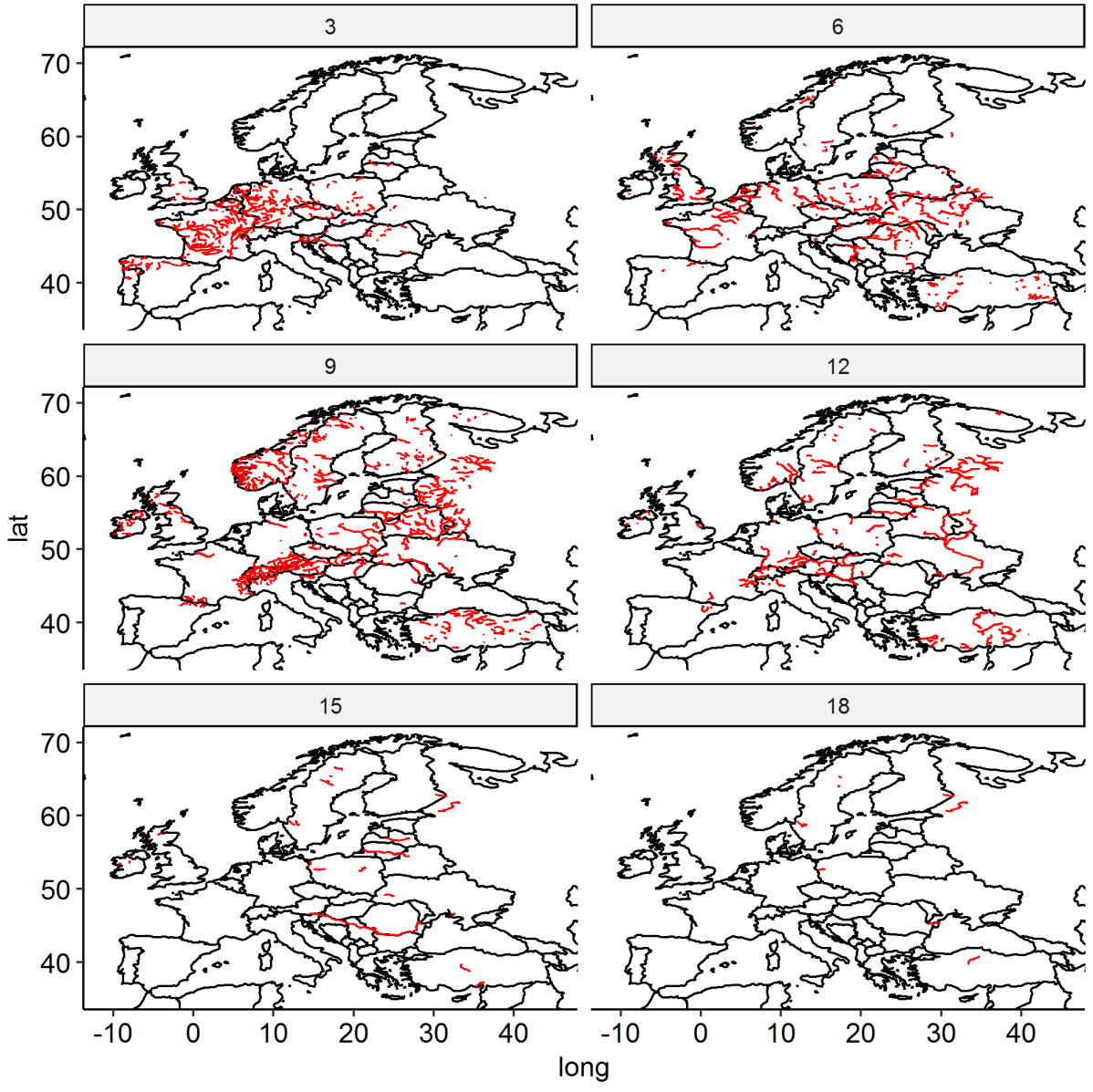

Figure 5. From a particular Pan-European event, snapshots (days since the start of the event) are displayed. Red points indicate the cells of the river network that were activated by the event.

Nat. Hazards Earth Syst. Sci. Discuss., https://doi.org/10.5194/nhess-2018-231
Manuscript under review for journal Nat. Hazards Earth Syst. Sci.
Discussion started: 14 August 2018

3.4 Event description

The pan-European event identification resulted in 428 events, which we aimed to describe by the discharge peaks of the events at 298 representative locations on the river network. However, the pan-European events did not yield discharge peaks at all representative locations for each events.

Where no event occurred (36% of the entries in the observed descriptor matrix), we had to fill the gaps by assigning auxiliary values. Per representative location (i.e. column-wise) we set up a number of local time windows in between the peaks of identified events, corresponding to the number of gaps between those respective peaks. Within each of these local time windows, we selected the maximum value as auxiliary value.

4 Multivariate statistical model

4.1 Marginal distributions

We fitted Generalised Pareto Distributions (GPDs) (Coles et al., 2001) to the upper tail of the marginal distributions, i.e. for each column in the observed descriptor matrix. The issue of threshold choice for GPDs is well-discussed in the literature (Northrop et al., 2017). After comparing the model fit, we used the $\zeta_m = 0.94$ empirical quantile as marginal threshold for the GPD at each location. This threshold was found by trial and error, where we tested the quality of the marginal GPD fits with a standard method, comparing the empirical quantiles and probabilities against the modelled, including checks of the tolerance intervals, see Fig.(6).

4.2 Multivariate dependence model

To be able to capture the dependence between sets of descriptors (i.e. rows in the observed descriptor matrix), we started by transforming the marginals to the uniform space. This transformation is applied in many other analyses, e.g. copulas (Genest and Favre, 2007; Nelsen, 2007). Values below the marginal threshold used to fit the GPDs in Sect.[4.1] were transformed using the empirical marginal distribution and values above the marginal threshold were transformed using the GPDs. We applied a model with two different components to capture the dependence structure, one for the non-extreme part and one for the extreme part.

The dependence structure of the non-extreme part was captured using a multivariate kernel density with Gaussian kernels. We transformed the (entire) uniform marginals to the normal space, with the mean $\mu = 0$ and the standard deviation $sd = 1$. Bandwidths for the kernels where selected using the method of Silverman (2018).

To capture the dependence of the extreme part we chose the model of Heffernan and Tawn (2004), hereafter referred to as 'HT04'. HT04 is a pair-wise dependence model that can be described as a method of lines, $Y_i = aY_{-i} + Y_{-i}^b Z$. Two HT04 model fits are required for each pair of marginals, with either marginal as the conditioning marginal Y_i and the other as the dependent marginal Y_{-i}. Each fit holds two parameters, a and b, after which a residual Z is calculated from each observed data point. The data used to fit the model are the pairs where the conditioning marginal Y_i is larger than a fitting threshold ζ_f.

Nat. Hazards Earth Syst. Sci. Discuss., https://doi.org/10.5194/nhess-2018-231
Manuscript under review for journal Nat. Hazards Earth Syst. Sci.
Discussion started: 14 August 2018

Natural Hazards and Earth System Sciences
Discussions

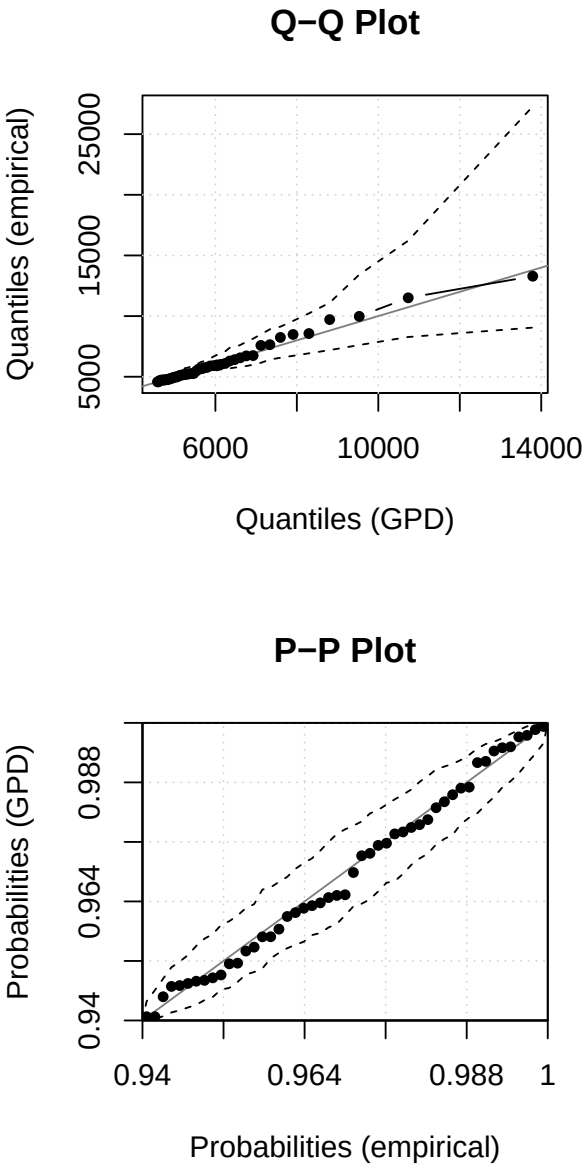

Figure 6. Standard visual checks of the 'goodness-of-fit' of the GPD. The dashed lines represent the 95% tolerance interval.

With an infinite number of samples drawn from HT04, each model fit would result in as many pair-wise lines as there are data points. However, for simulation a subset of these lines is used, since HT04 should be applied only if the largest marginal in the set is above a particular simulation threshold .

Nat. Hazards Earth Syst. Sci. Discuss., https://doi.org/10.5194/nhess-2018-231
Manuscript under review for journal Nat. Hazards Earth Syst. Sci.
Discussion started: 14 August 2018

Natural Hazards and Earth System Sciences
Discussions

To fit HT04, we transformed the (entire) uniform marginals to the Laplace space (Keef et al., 2013). We obtained HT04 model fits in the Laplace space using maximum likelihood, with each marginal as conditioning variable and all other marginals as dependent variables, resulting in a total of 298*297 model fits, where we chose the fitting threshold $\zeta_f = 0.9$, which was a trade-off between variance and bias. HT04 was recently applied for fluvial flooding (Keef et al., 2009; Lamb et al., 2010; Wyncoll et al., 2013) and for coastal flooding (Wyncoll and Gouldby, 2015; Gouldby et al., 2017), in which the model fitting procedure is described in more detail.

4.3 Simulation

We split the observed uniform descriptor matrix into a 'non-extreme' part, and an 'extreme' part. Each row in which not a single descriptor exceeded an extremal simulation threshold $\zeta_e = 0.98$ was determined to be non-extreme (23%), the rest (77%) was determined to be extreme (somewhere). For the non-extreme sets, we re-sampled from the non-parametric model. For the extreme sets, we re-sampled from HT04, where the model fit was used of the marginal that was the largest by quantile in the set. All sets were re-sampled $N = T_{sim}/T_{obs}$ times, where T_{obs} is the duration of the observed data (25 years) and T_{sim} is the duration of the synthetic data (10.000 years). After the simulation, we transformed the marginals of the synthetic descriptor matrix to respect the fitted GPDs, thereby slightly distorting the dependence structure.

4.4 Validation

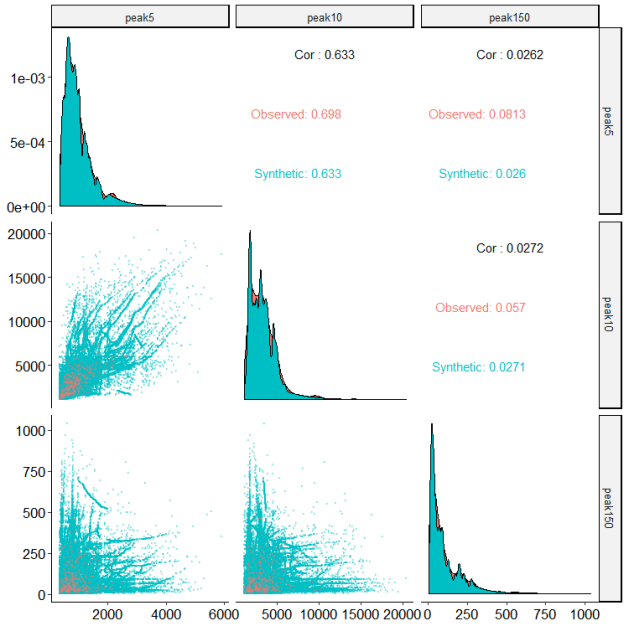

Figure 7. Pair-wise plots of three descriptors. Red is the observed data and blue is the simulated data.

Nat. Hazards Earth Syst. Sci. Discuss., https://doi.org/10.5194/nhess-2018-231
Manuscript under review for journal Nat. Hazards Earth Syst. Sci.
Discussion started: 14 August 2018

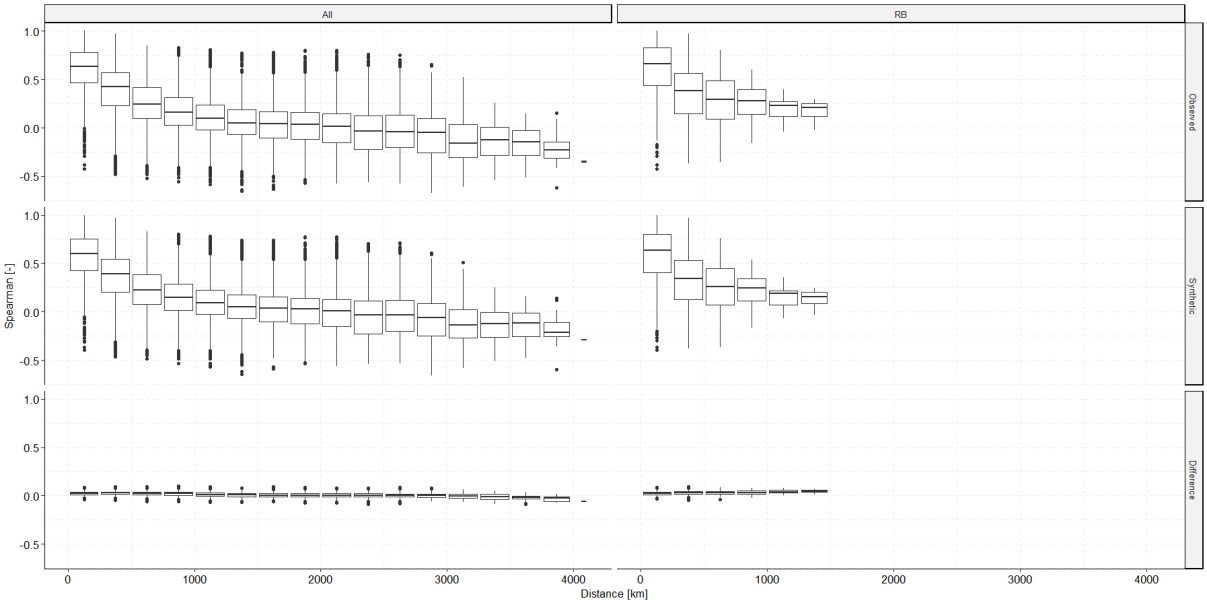

Figure 8. Spatial correlation structure of the observed descriptors versus the synthetic descriptors, summarised by pair-wise Spearman correlation. The upper panel shows the correlation in the observed data, the middle panel shows the correlation in the synthetic data and the lower panel shows the difference between the observed and the synthetic correlation for each pair. The left column shows the correlation between all pairs of locations, right shows only the pairs that are in the same river basin.

Using multivariate extreme value analysis, we extended the observed descriptor matrix with synthetic data, obtaining a (large) synthetic descriptor matrix. The patterns in the larger synthetic descriptor matrix had to match the patterns found in the smaller observed descriptor matrix. We focused on two main patterns; marginal distributions (a column-wise pattern) and dependence structure (a row-wise pattern). To respect the fitted marginal distributions and, simultaneously, retain the dependence structure is challenging. There is no perfect method for these two objectives. We chose to respect the fitted distributions and so we had to compare the dependence structure in the observed data with the synthetic.

A sample of the observed descriptors versus the synthetic descriptors is shown in Fig.(7). It can be observed that we managed to capture the dependence structure reasonably well, as the simulated descriptors follow the trends in the observed data. Fig.(8) shows the pair-wise, spatial correlation structure between descriptors at different locations. Rather than choosing distance along the river branch, we chose geospatial distance such that we could compare locations not only within river basins, but also across different river basins. The Spearman correlation coefficients of the observed descriptors and the synthetic descriptors agree very well, which indicates that the general spatial dependence structure is similar in the observed descriptor matrix and in the synthetic descriptor matrix. The difference indicates an overall slightly higher (positive or negative) correlation in the observed descriptor matrix. A shift from positive to negative correlation can be observed around $2000 - 2500km$, which may be related to large-scale atmospheric patterns. Following up on the general check of correlation between the entire descriptor sets, we specifically checked if we managed to capture the tail-end correlations. Fig.(9) shows that the general behaviour of co-

Nat. Hazards Earth Syst. Sci. Discuss., https://doi.org/10.5194/nhess-2018-231
Manuscript under review for journal Nat. Hazards Earth Syst. Sci.
Discussion started: 14 August 2018

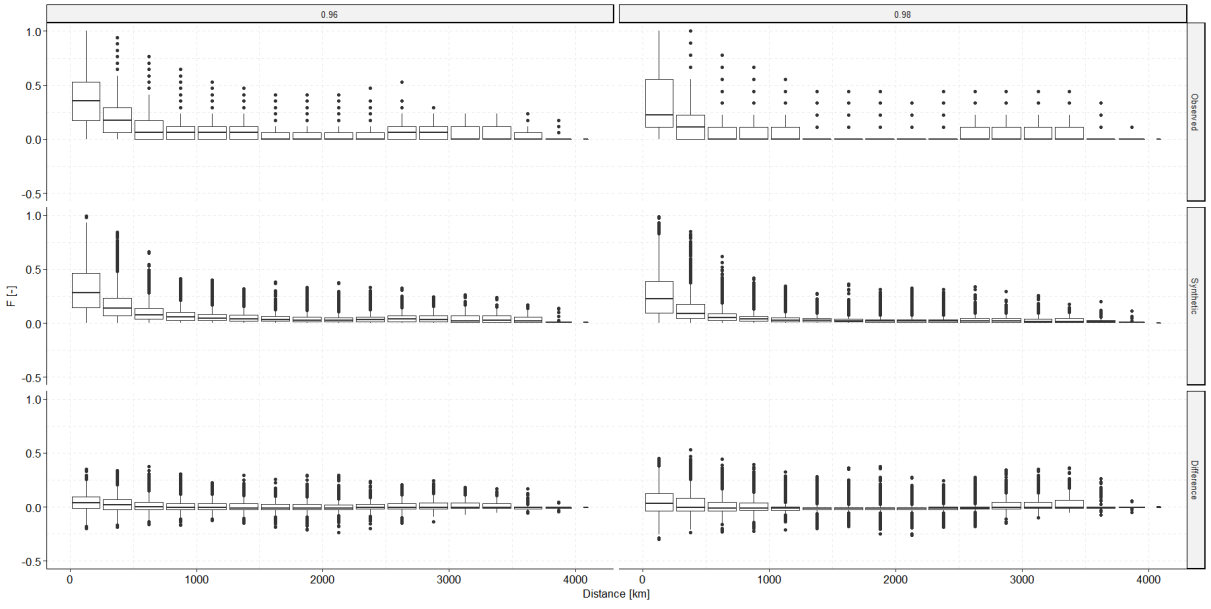

Figure 9. Pair-wise comparison of the tail-end of the marginals for all 298 locations. For a selection of high quantiles we counted the fraction F of events where extremes at both locations exceeded the respective quantile divided by the total number of quantile exceedances. The upper panel shows the fractions in the observed data, the middle panel shows the fractions in the synthetic data and the lower panel shows the pair-wise difference between the observed and the synthetic fractions.

occurrence of extremes was relatively well captured in the dependence model. The general pattern in the synthetic descriptors is reasonably similar to the pattern in the observed descriptors. A small positive bias can be observed, which shows that the dependence model slightly underestimated the frequency of joint occurrence of extremes. The zero difference generally falls within the lower quartile. Moreover, the higher the quantile for which we checked the exceedance, the fewer quantile exceedances to count, which lead to a larger spread in the difference between the observed and the synthetic set.

5 Conclusions

We used a new 'noise removal' method, with which we successfully tracked discharge waves in all major European river basins and clustered these river basin events to pan-European events using a global time window. With two multivariate dependence models, we managed to capture the dependence structure between discharge peaks of daily discharge at 298 different locations on the river network of major European rivers. We created a synthetic data set, comprising 10.000 years of synthetic peak sets with a similar dependence structure as in the observed discharge peaks, thereby showing spatially coherence. This data set will be used to generate discharge hydrographs to drive a European-wide inundation model for large-scale, flood risk assessment.

Competing interests. The authors declare that they have no conflict of interest.

Acknowledgements. We would like to thank the European Joint Research Centre for providing the European discharge data set. This research is part of the 'system-risk' project and has received funding from the European Union's Horizon 2020 research and innovation programme under the Marie Skłodowska-Curie grant agreement No 676027.

Nat. Hazards Earth Syst. Sci. Discuss., https://doi.org/10.5194/nhess-2018-231
Manuscript under review for journal Nat. Hazards Earth Syst. Sci.
Discussion started: 14 August 2018

References

Alfieri, L., Salamon, P., Bianchi, A., Neal, J., Bates, P., and Feyen, L.: Advances in pan-European flood hazard mapping, Hydrological Processes, 28, 4067–4077, 2014.

Berthet, L., Andréassian, V., Perrin, C., and Javelle, P.: How crucial is it to account for the antecedent moisture conditions in flood forecasting? Comparison of event-based and continuous approaches on 178 catchments, Hydrology and Earth System Sciences, 13, 819–831, 2009.

Borgomeo, E., Farmer, C. L., and Hall, J. W.: Numerical rivers: A synthetic streamflow generator for water resources vulnerability assessments, Water Resources Research, 51, 5382–5405, 2015.

Boughton, W. and Droop, O.: Continuous simulation for design flood estimation—a review, Environmental Modelling & Software, 18, 309–318, 2003.

Cameron, D., Beven, K. J., Tawn, J., Blazkova, S., and Naden, P.: Flood frequency estimation by continuous simulation for a gauged upland catchment (with uncertainty), Journal of Hydrology, 219, 169–187, 1999.

Coles, S., Bawa, J., Trenner, L., and Dorazio, P.: An introduction to statistical modeling of extreme values, vol. 208, Springer, 2001.

Desai, B., Maskrey, A., Peduzzi, P., De Bono, A., and Herold, C.: Making Development Sustainable: The Future of Disaster Risk Management, Global Assessment Report on Disaster Risk Reduction, 910; 333.7-333.9, United Nations Office for Disaster Risk Reduction (UNISDR), https://archive-ouverte.unige.ch/unige:78299, iD: unige:78299, 2015.

Dottori, F., Salamon, P., Bianchi, A., Alfieri, L., Hirpa, F. A., and Feyen, L.: Development and evaluation of a framework for global flood hazard mapping, Advances in water resources, 94, 87–102, 2016.

Falter, D., Schröter, K., Dung, N. V., Vorogushyn, S., Kreibich, H., Hundecha, Y., Apel, H., and Merz, B.: Spatially coherent flood risk assessment based on long-term continuous simulation with a coupled model chain, Journal of Hydrology, 524, 182–193, 2015.

Field, C. B.: Managing the risks of extreme events and disasters to advance climate change adaptation: special report of the intergovernmental panel on climate change, Cambridge University Press, 2012.

Genest, C. and Favre, A.-C.: Everything you always wanted to know about copula modeling but were afraid to ask, Journal of hydrologic engineering, 12, 347–368, 2007.

Gouldby, B., Wyncoll, D., Panzeri, M., Franklin, M., Hunt, T., Hames, D., Tozer, N., Hawkes, P., Dornbusch, U., and Pullen, T.: Multivariate extreme value modelling of sea conditions around the coast of England, in: Proceedings of the Institution of Civil Engineers-Maritime Engineering, vol. 170, pp. 3–20, 2017.

Heffernan, J. E. and Tawn, J. A.: A conditional approach for multivariate extreme values (with discussion), Journal of the Royal Statistical Society: Series B (Statistical Methodology), 66, 497–546, 2004.

Jongman, B., Hochrainer-Stigler, S., Feyen, L., Aerts, J. C., Mechler, R., Botzen, W. W., Bouwer, L. M., Pflug, G., Rojas, R., and Ward, P. J.: Increasing stress on disaster-risk finance due to large floods, Nature Climate Change, 4, 264, 2014.

Keef, C., Tawn, J., and Svensson, C.: Spatial risk assessment for extreme river flows, Journal of the Royal Statistical Society: Series C (Applied Statistics), 58, 601–618, 2009.

Keef, C., Papastathopoulos, I., and Tawn, J. A.: Estimation of the conditional distribution of a multivariate variable given that one of its components is large: Additional constraints for the Heffernan and Tawn model, Journal of Multivariate Analysis, 115, 396–404, 2013.

Lamb, R., Keef, C., Tawn, J., Laeger, S., Meadowcroft, I., Surendran, S., Dunning, P., and Batstone, C.: A new method to assess the risk of local and widespread flooding on rivers and coasts, Journal of Flood Risk Management, 3, 323–336, 2010.

Nelsen, R. B.: An introduction to copulas, Springer Science & Business Media, 2007.

Northrop, P. J., Attalides, N., and Jonathan, P.: Cross-validatory extreme value threshold selection and uncertainty with application to ocean storm severity, Journal of the Royal Statistical Society: Series C (Applied Statistics), 66, 93–120, 2017.

Paprotny, D., Morales-Nápoles, O., and Jonkman, S. N.: Efficient pan-European river flood hazard modelling through a combination of statistical and physical models, Natural Hazards and Earth System Sciences, 17, 1267, 2017.

Schröter, K., Kunz, M., Elmer, F., Mühr, B., and Merz, B.: What made the June 2013 flood in Germany an exceptional event? A hydro-meteorological evaluation, Hydrology and Earth System Sciences, 19, 309–327, 2015.

Silverman, B. W.: Density estimation for statistics and data analysis, Routledge, 2018.

Vorogushyn, S., Merz, B., Lindenschmidt, K.-E., and Apel, H.: A new methodology for flood hazard assessment considering dike breaches, Water Resources Research, 46, 2010.

Vorogushyn, S., Bates, P. D., de Bruijn, K., Castellarin, A., Kreibich, H., Priest, S., Schröter, K., Bagli, S., Blöschl, G., Domeneghetti, A., et al.: Evolutionary leap in large-scale flood risk assessment needed, Wiley Interdisciplinary Reviews: Water, 5, 2018.

Vousdoukas, M. I.: Developments in large-scale coastal flood hazard mapping, Natural Hazards and Earth System Sciences, 16, 1841, 2016.

Ward, P. J., Jongman, B., Weiland, F. S., Bouwman, A., van Beek, R., Bierkens, M. F. P., Ligtvoet, W., and Winsemius, H. C.: Assessing flood risk at the global scale: model setup, results, and sensitivity, Environmental Research Letters, 8, 044 019, http://stacks.iop.org/1748-9326/8/i=4/a=044019, 2013.

Winsemius, H. C., Aerts, J. C., van Beek, L. P., Bierkens, M. F., Bouwman, A., Jongman, B., Kwadijk, J. C., Ligtvoet, W., Lucas, P. L., van Vuuren, D. P., et al.: Global drivers of future river flood risk, Nature Climate Change, 6, 381, 2016.

Wyncoll, D. and Gouldby, B.: Integrating a multivariate extreme value method within a system flood risk analysis model, Journal of Flood Risk Management, 8, 145–160, 2015.

Wyncoll, D., Gouldby, B., and Hames, D.: Application of a conditional approach for multivariate extreme values to flood risk, EVAN 2013, p. 87, 2013.